International Journal of Architectural, Civil and Construction Sciences
ISSN: 2415-1734
Vol:12, No:11, 2018

Three-Dimensional Numerical Investigation for Reinforced Concrete Slabs with Opening

Abdelrahman Elsehsah, Hany Madkour, Khalid Farah

***Abstract*—**This article presents a 3-D modified non-linear elastic model in the strain space. The Helmholtz free energy function is introduced with the existence of a dissipation potential surface in the space of thermodynamic conjugate forces. The constitutive equation and the damage evolution were derived as well. The modified damage has been examined to model the nonlinear behavior of reinforced concrete (RC) slabs with an opening. A parametric study with RC was carried out to investigate the impact of different factors on the behavior of RC slabs. These factors are the opening area, the opening shape, the place of opening, and the thickness of the slabs. And the numerical results have been compared with the experimental data from literature. Finally, the model showed its ability to be applied to the structural analysis of RC slabs.

***Keywords*—**3-D numerical analysis, damage mechanics, RC slab with opening.

I. Introduction

EVEN with the remarkable research efforts and contributions, the task of nonlinear simulation of concrete structures is still inspiring. Various used theories for the nonlinear modeling of concrete are plasticity, fracture-based approaches, and continuum damage mechanics (CDM).

Various Continuum Damage model has been built based on various rigorous basis using thermodynamic and micromechanics for representing the deterioration of mechanical properties and the geometrical phenomena. Moreover, the nonlinear behavior of RC structures depends mainly on the initiation, evolution, and coalescence of microcracks.

Consequently, the energy imparted during the nucleation and growth of microcracks and coalescence into microcracks have been described with the help of continuum damage mechanics.

There are a lot of ways to understand the behavior of RC slabs. Experimental tests are widely implemented and dependable methods to understand the behavior of RC slabs. Experimental methods are dependent on various conditions. While numerical methods save money and time; hence, it becomes popular in the recent years.

Koh et al. [1] have experimented five slabs with dimensions of 1100 mm length X 300 width mm X 75 mm thickness and a central rectangular opening with dimension 300 mm length X 150 mm width. All slabs were reinforced with eight steel reinforced bars of diameter 10 mm. Based on their experimental results, they concluded that the reduction of 15% area due to the rectangular opening located at the center of RC slabs reduces 36.6% of flexural strength.

Enochsson [2] conducted an experimental work on two-way RC slabs to investigate the effect of opening area on slabs. This investigation included slabs with large and small openings. It was concluded that the characteristics of reference slab (without opening) and the slab with a small opening was nearly equal, while the slab with large opening had a dramatic deterioration of its capacity. Also, the ultimate load was decreased by about 74%.

Wissam [3] tested six RC slabs with dimensions 1400 mm length X 450 mm width X 90 mm thickness with three different square openings (150 mm, 200 mm, and 250 mm) and the other with different shape of opening with constant area (square, rectangle and circle) with opening ratio 7.4%. Test results showed that RC slabs with the same constant area nearly have the same behavior as the ultimate load capacity is decreased by 50.0%, 50.15% and 49.56% for square, rectangle and circle respectively and the ultimate load capacity of RC slabs with opening ratio 4.2%, 7.4% and 11.6% is decreased by 46.37%, 50.0% and 59.01%, respectively.

A numerical program had been conducted by Hosam [4] who used Finite Element Analysis (FEA) by using ANSYS 5.4 program with a nonlinear concrete method of a complex support conditions to predict the ultimate loads of different kinds of slabs. It was chosen the support condition as the parameter of the study. The results showed that the deflection of the slabs with opening that fixed on all four sides was about 5.6% of that simply supported on the all four sides. Also, the deflection of slabs, that are fixed at two opposite sides and fixed-free at the other two sides, was about 9.6 % of that simply supported at two opposite sides. The value of normal stresses distributions was greatly affected by opening in slabs especially at the opening zone.

Chee et al. [5] used the yield line method for studying a simply-supported and fixed end for square slabs with cutouts at ultimate limit state. They concluded that a simply-supported slab would have a reduction in ultimate area load of up to 11% and a reduction of ultimate total load of up to 19% since most of the slabs have small opening with size which is 0.3 times the slab dimension, while the fixed-end slab would have insignificant reduction in both ultimate total load and ultimate area load capacities of 7% and 4%, respectively.

Anjaly and Preetha [6] examined the structural behavior of ribbed flat slabs with and without openings and the effect of locations and openings sizes on the ultimate loads. These slabs were analyzed by using finite element software. They concluded that opening locations and its dimensions have a major effect in the structural behavior of ribbed flat. The size

Abdelrahman Elsehsah is with the Aswan University, Egypt (e-mail: abdelrahman.elsehsah@gmail.com).

of openings in the intersection between by two column strips should not be exceeded by 10% of the column strip width, while for the intersection region between a column strip and a middle strip, size limit is 20% of the column strip width. But, for the intersection region between by two middle strips, no limitation has been found in opening size even it reaches up to 40% of the width of column strip.

American Concrete Institute (ACI) code [7] gave limitations and guidelines for opening location and size. If the designer satisfies those requirements, the analysis could be waived. Modifications to an existing structure are not frequent but it is occurred according to user's requirements. New slab openings or cut-outs in an existing concrete building are easily accommodated in the majority of instances. The purpose of these guidelines and limitations are to offer the structural engineer on selecting locations and sizes for openings in for both new and existing structures.

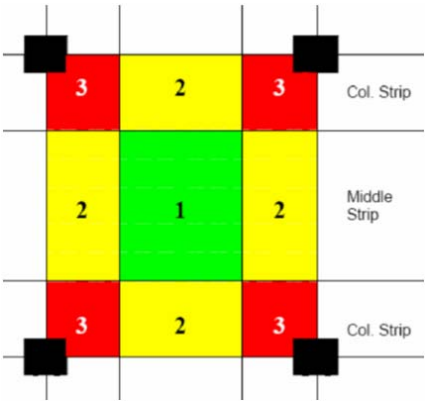

Fig. 1 Suggested opening locations according to ACI [7]

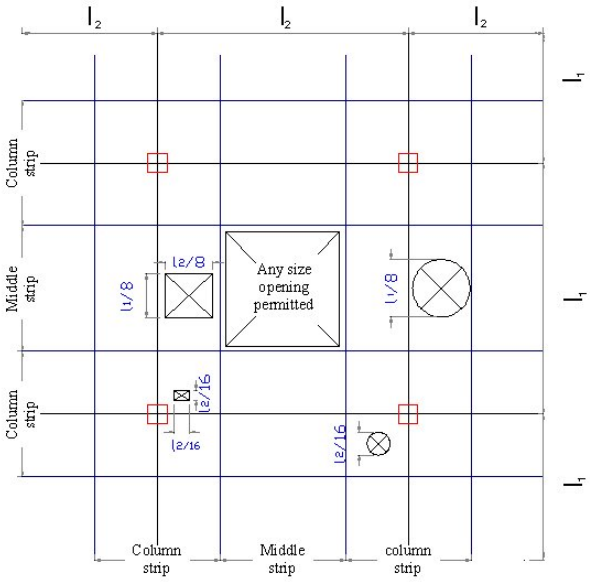

Fig. 2 Suggested opening area according to the Egyptian Code [8]

Fig. 1 illustrates the areas that are suggested where the openings can be made; any openings in area 3 should be avoided as much as possible, but if there is a need to make an opening in this area, the suggested opening size should not be larger than 30 cm; it should be noticed that openings in this area could reduce the critical section considered for resisting punching-shear as explained in ACI 318-02. The intersection between column and middle strips (area 2) is less critical than area 3. So, the suggested openings having a width less than 15 percent of the span length can be made in this area.

Egyptian code [8] put guidelines for making openings in flat slab. It is possible to make cut-outs in the intersection between two middle strips; the maximum dimension of the opening is equal to 0.4 of the spans. Meanwhile, for the intersection between a column strip and middle strip; openings in the intersection between column strip and middle strip can be cut with dimensions up to one-quarter of the span. Lastly for opening in the intersection area of two column strips, the maximum dimension of the opening is equal to 0.1 of the span.

II. Scope and Objective

Opening in RC slabs is usually used in the existing floors to accommodate new ducts, elevators and escalators, etc. Because of this opening, there is a deterioration in the shape of cracks happen in the concrete and/or stress concentration. So, from the structural point of view, the better place to create an opening is the place which has the least value of the stresses. Unfortunately, architectural and functional requirements often cause them to be in different positions irrespective to the resulted stresses. Hence in some cases, it is a must to make an opening in the slab regardless stated in the different RC codes. So, it is vital to better understanding the behavior of RC slabs with opening and the evolved damage and stresses.

This research work aims to investigate the structural behavior of RC slabs and its deterioration that happens due to creating opening by explaining the damage growth, the ultimate load and failure modes. Twenty RC slabs in five groups with different parameters are investigated as: opening area, opening shape, number of slab opening, opening places and slab thickness.

This numerical investigation will be carried out by the modified nonlinear elastic damage model. The modified theory considered the nonlinear behavior and the gradual degradation of the elastic stiffness caused by the existing damaged state in addition to the nucleation and growth of microcracks.

This research article is presented into four sections (after the introduction and the scope). The first section is the numerical modeling which discusses the main key concepts of the proposed nonlinear elastic- damage model with and presentation of the modified Helmholtz free-energy function. The next section introduces the numerical program which deals with the used material properties, modelling of elements and the categorization of the studied slabs with the investigated parameters. The following section is the test results and analysis which illustrate the behavior of the slabs from different points views, as load-deflection, ultimate load,

stress and damage distribution. Finally, concluded remarks are tabulated in the final section.

III. Numerical Modelling

The current research work was a modification for the developed non-linear elastic damage theory introduced by Madkour [7]. This theory focused on simulating the deterioration and damage mechanism based on the stored and dissipated energies in terms of the internal state variables with the help of irreversible thermodynamics.

A. Damage Non-Linear Elastic Model

The current numerical damage model is a modification of the developed nonlinear elastic damage theory [8] that has been developed for simulating the nonlinearity of the deteriorated concrete structures. The current damage model presents a rational constitutive model that considers the nonlinear behavior of concrete and damage evolution through both stored and dissipated energies in terms of the internal state variables based on irreversible thermodynamics. The new model considers the specific characteristics of the dilatational response of concrete to accurately reproduce the behavior of RC elements. Moreover, concrete has been assumed to exhibit nonlinear stable elastically (only hardening behavior is under consideration). The proposed elasticity tensor will be considered as a one-parameter damage-dependent tensor by tensorial algebra and thermodynamic requirements, as:

$$\tilde{D}_{ijkl} = \lambda\phi_{ij}\phi_{kl} + \mu(\phi_{ik}\phi_{jk} + \phi_{il}\phi_{jk}) \tag{1}$$

$\tilde{D}_{ijkl}$ is the fourth-order elastic, and λ, μ are the Lame's constants for virgin material. The function ϕ_{ij} includes the damage state Ω, and a material constant m has been proposed, as:

$$\phi_{ij} = \delta_{ij} - m\Omega_{ij} - (1-m)\Omega_{im}\Omega_{mj} \qquad 0 \le m \le 1 \tag{2}$$

The material constant m is used to reflect degree of the damage influence on D_{ijkl} matrix.

B. Modified Helmholtz Free-Energy Function

The new proposed Helmholtz free-energy function Ψ as a thermodynamic potential, has been developed to be convex function of all observable and internal variables and will be proposed into elastic potential function and dissipative parts, as follows:

$$\Psi = \Psi^{ed} + \Psi^{ned} - \Psi^{dila} - \Psi^{S} \tag{3}$$

The term Ψ^{ed} refers to the classical elastic strain energy stored in the material during the loading process. The thermodynamic elastic damaged free-energy Ψ^{ed} has been introduced by [9] in the term of total strain ε, as:

$$\Psi^{ed} = \frac{1}{2}\varepsilon_{ij} : D_{ijkl} : \varepsilon_{kl} \tag{4}$$

Ψ^{ned} characterizes the nonlinear Elastic-Damage potential function, that refers to the strain energy dissipated in the material during the loading process, as well as to produce the nonlinear relation between the thermodynamic conjugate force R and the damage variable Ω, as:

$$\Psi^{ne} = \frac{1}{3}\varepsilon_{ij} : \tilde{D}_{ijkl} : \varepsilon_{km} : \varepsilon_{ml} \tag{5}$$

Dragon et al. [10] have introduced the dissipated energy due to dilatancy phenomena. Furthermore, this dissipated energy Ψ^{dila} has been introduced to simulate the damage evolution depending on the hydrostatic stress and to characterize the splitting mode in the level of free-energy function as:

$$\Psi^{dila} = G.\Omega_{ij} : P^{+}_{ijkl} : \varepsilon_{kl} \tag{6}$$

where G is a material constant relevant to damage-induced residual stresses. P^{+}_{ijkl} is the fourth-order transformation tensor which will be determined, according to [11], considering the states of the current strain tensor, as:

$$P^{+}_{ijkl} = Q^{+}_{ia}Q^{+}_{jb}Q_{ka}Q_{lb} \tag{7}$$

where Q_{ij} and Q^{+}_{ij} are the regular and positive (tensile) spectral projection tensors, respectively and can be defined, as:

$$Q_{ij} = \sum_{k=1}^{3} p_i^{(k)} p_j^{(k)} \tag{8}$$

$$Q^{+}_{ij} = \sum_{k=1}^{3} H^{d}(\varepsilon_k) p_i^{(k)} p_j^{(k)} \tag{9}$$

where $(0 \le H^{d}(\varepsilon_k) \le 1)$ is a Heaviside function depending on material constants. Consequently, the concept of the transformation tensor is essentially defined by the state of strain. The proposed expression for the Heaviside function will be introduced, as:

$$H^{d}(\varepsilon_i) = \begin{cases} 1 & \text{if } \varepsilon_i > 0 \\ H^{d} & \text{otherwise} \end{cases} \tag{10}$$

This function is described based on the state of strain with the material parameter (H^{d}).

The growth and propagation of damage continually produce

new micro-fractured surfaces within the material, which in fact represent an energy release process [12]. The fourth part of the free-energy expression in (3) has been introduced to characterize the dissipated surface energy due to the damage evolution process and takes the following form [13], as:

$$\Psi^{S} = \frac{1}{2} T^{d} . s^{2} \tag{11}$$

where T^d is a material constant and S is a scalar hardening variable describes the further development of the damage. Substitution from (4)-(6) and (11) in (3), the simple postulated Helmholtz free-energy function will be:

$$\Psi = \frac{1}{2}\varepsilon_{ij} : \tilde{D}_{ijkl} : \varepsilon_{kl} + \frac{1}{3}\varepsilon : \tilde{D}_{ijkl} : \varepsilon_{km} : \varepsilon_{ml} - G.\varepsilon_{ij} : P^{+}_{ijkl} : \Omega_{kl} - \frac{1}{2} T^{d} s^{2} \tag{12}$$

ε and Ω are the total strain and the damage variable, respectively.

C. Constitutive Equation

The constitutive equation and the kinetic equations will be derived by means of the well-established thermodynamic principles of irreversible processes. Clausius-Duhem inequality requires "the dissipation rate to be a non-negative quantity". Hence, the new constitutive relation can be established, as:

$$\sigma_{ij} = \frac{\partial \Psi}{\partial \varepsilon_{ij}} = \tilde{D}_{ijkl} : \varepsilon_{kl} + \tilde{D}_{ijkl} : \varepsilon_{km} : \varepsilon_{ml} - G.P^{+}_{ijkl} : \tilde{\Omega}_{kl} \tag{13}$$

The previous stress-strain formulation has the ability to simulate the linear and nonlinear behavior through the first and second terms, respectively. In addition, the formation of the splitting-like cracks will be the introduced dilatation concept, as well.

D. Dissipative Potential Surface

In (12), a new general free-energy function has been developed including damage tensor and the total (elastic) deformations. The second-order symmetric tensor R_{ij} of the damage conjugate force will be derived, as:

$$R_{ij} = -\partial \Psi / \partial \Omega_{ij} = -\frac{\partial \Psi^{ed}}{\partial \Omega_{ij}} - \frac{\partial \Psi^{ned}}{\partial \Omega_{ij}} + \frac{\partial \Psi^{dila}}{\partial \Omega_{ij}} \tag{14}$$

$$R_{ij} = (\lambda + 2\mu)\left[\varepsilon_{ij} : \phi_{ij} : N_{kl} : \varepsilon_{kl} + \frac{2}{3}\varepsilon_{ij} : \phi_{ij} : N_{kl} : \varepsilon_{km} : \varepsilon_{ml} \right] + G.P^{+}_{ijkl} : \varepsilon_{kl} \tag{15}$$

where ϕ_{ij} presented in (2) and N_{kl} can be derived, as:

$$N_{ij} = \partial \phi_{ij} / \partial \tilde{\Omega}_{ij} = -\left[m + 2(1-m).\tilde{\Omega}_{ij} \right] \tag{16}$$

Moreover, the formation of the damage surface will cause energy dissipation due to further development of damage. The thermodynamic force S conjugated to the development of the damage surface can be obtained, as

$$S = -\frac{\partial \Psi}{\partial s} = -T^{d} . s \tag{17}$$

The proposed damage surface F^d that governs the direction of dissipative fluxes and functions in the tensorial formation of the thermodynamic damage force is defined, as:

$$F^{d} = S^{d}\left[\sqrt{R_{ij} . R_{ij}} + tr(\tilde{\Omega}).tr(R) \right] - (S_0 + \Delta s) \tag{18}$$

where S^d is a material constant controlling the damage surface size, S_0 represents the initial damage threshold, and ΔS is a parameter to simulate the evolution of damage surface.

E. Damage Evolution

The damage direction and growth are described by a damage dissipation surface, expressed in terms of the thermodynamic conjugate force. So, the growth of damage internal variable will be, as:

$$\dot{\Omega}_{ij} = dz^{d} . (\partial F^{d} / \partial R_{ij}) \tag{19}$$

The proposed model used Valanis concept of intrinsic time [14] to introduce the damage evolution law based on the total strain history. The definition of the intrinsic time z^d which was postulated, as:

$$dz^{d} = d\xi / f \; ; \quad f = 1 + \beta\xi + \frac{1}{2}\beta\xi^{2} \tag{20}$$

β is a positive constant for hardening material, f is a nonlinear hardening function, and ξ is the intrinsic measure. And this measure will be defined in the strain space according to the endochronic theory [14], as:

$$d\xi = \left| de^{pd}_{ij} \right| = \sqrt{de^{pd}_{ij} de^{pd}_{ij}} \; ; \quad e^{pd}_{ij} = \varepsilon^{pd}_{ij} - 1/3.\delta_{ij}\varepsilon^{pd}_{kk} \tag{21}$$

Therefore, in the proposed model, the damage threshold has been formulated basically on the total nonlinear deformation history of the material.

IV. Numerical Program

A. Material Properties

The constitutive model for concrete has been considered as a non-linear elastic and the plastic response is assumed to be neglected. The constitutive model for steel is assumed to be ideal elastic. Full bond between steel and concrete is

presented. All the mechanical properties of the used materials are presented in Table I.

TABLE I
MECHANICAL PROPERTIES OF CONCRETE AND STEEL REINFORCEMENT BARS

Concrete	E	(25.0X 10^6) kN/M^2
	Poisson's ratio	0.22
	Fcu	(25.0 X 10^3) kN/M^2
Steel Reinforcement m	Fy	(4.7 X 10^5) kN/M^2
	Fu	(7.3X 10^5) kN/M^2

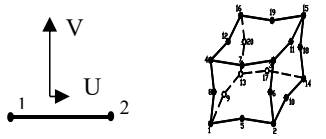

(a) (b)

Fig. 3 The used finite element (a) Elastic bar element (two-node element), (b) Isoparametric Quadratic element (20-node element)

B. Element Modelling

The numerical investigation was carried out using Finite Element (FE) Code FINAL [15]. In the FINAL analysis, perfect bond is assumed between the concrete and the reinforced steel bars. In this research, the developed numerical modelling to illustrates the deterioration that happened in the RC slabs with openings, two types of finite elements [9] are used to simulate concrete material and steel reinforcement which are; Isoparametric Quadratic element (20 nodes element) and elastic bar element (two-node element), respectively as illustrated in Fig. 3.

C. The Parametric Program

The proposed numerical model has been applied for simulating and predicting the complex behavior of RC slab with and without openings and the dimensions are, as shown in Fig. 2. All RC slabs have been numerically tested in two third points loading with (200 mm from the center along X-axis on both sides), RC slabs for Group I and Group II have reinforcement details; 3Φ10 mm and 8Φ10 mm in the longitudinal and transverse directions respectively, while for Group III and Group IV have reinforcement details; 8Φ10 mm and 8Φ10 mm respectively. The numerical program is categorized into four groups, as follows:

- **Group I**: - this group includes four RC slabs; the first slab is acting as a control slab (without opening). The other three slabs were investigated numerically and compared with the experimental results [16] to investigate the effect of area opening on the behavior of RC slabs,
- **Group II**: - It contains three slabs; a control slab and the rest were examined numerically to investigate the effect of shape of opening,
- **Group III**: - Eight RC slabs were analyzed numerically to investigate the effect of place opening.
- **Group IV**: Three RC slabs to evaluate the effect of opening place, three slabs have been analyzed numerically.

TABLE II
NUMERICAL PROGRAM

Group	Slab No.	Dimension	Shape of opening	place of opening	Dimension of opening	Slab Thickness	Investigated Parameter
I	S1.0	1400 mm X 500 mm	----	----	----	100 mm	Opening Area
	S1.1		Square	At the center	100 mm X 100 mm		
	S1.2		Square	At the center	200 mm X 200 mm		
	S1.3		Square	At the center	300 mm X 300 mm		
II	S2.0	1200 mm X 400 mm	----	----	----	200 mm	Shape of Opening
	S2.1		Rectangle	At the center	400 mm X 200 mm		
	S2.2		Square	At the center	285 mm X 285 mm		
III	S3.0.1	1800 mm X 1800 mm	----	----	----	200 mm	Slab Thickness
	S3.1.1		Square	At the center	200 mm X 200 mm		
	S3.0.2		----	----	----	150 mm	
	S3.2.2		Square	At the center	200 mm X 200 mm		
	S.3.0.3		----	----	----	120 mm	
	S3.3.3		Square	At the center	200 mm X 200 mm		
	S3.0.4		-----	-----	-----	100 mm	
	S3.4.4		Square	At the center	200 mm X 200 mm		
IV	S4.0	2000 mm X2000 mm	----	-----	----	200 mm	Place of Opening
	S4.1		Square	At the center	400 mm X 400 mm		
	S4.2		Square	At the corner	400 mm X 400 mm		

V. RESULTS AND ANALYSIS

Table III lists the detailed results; resulting cracking load, ultimate load and the maximum induced deflections for each tested beam. The numerical results can be analyzed, as follows:

A. Load-Deflection Behavior

Regarding to Load-deflection curves as it displayed in Figs. 4-7 and Table III, it is concluded that when a RC slab is subjected, the deflection increases with the load linearly in an elastic manner. After that the cracks start to develop and the

deflection increases at fast rate. After the developing of cracks, the load deflection curve is about nonlinear up to the yielding of the flexural reinforcement; after that the deflection stays to increase without a significant increment in load. The load-deflection curves are groups according to opening area, shape of opening, slab thickness and place of opening which are the fundamental variables of this study and also presented in Figs. 4-7.

From the load-deflection curves as displayed in Fig. 4 and Table III, it was concluded that when introducing opening in RC slab with different areas which represent 1.4%, 5.7%, and 12.8 for slabs S1.1, S1.2 and S1.3, respectively, the ultimate load capacity decreased about 48.7%, 49.3%, and 56.1% respectively in a comparison with the control slab without opening S1.0. In addition to the reduction in the stiffness of the slab, consequently the ultimate load will decrease.

Regarding the opening shape in Group II as presented in Fig. 5 and Table III, slabs S2.1 and S2.2 (which have the same opening area ratio 16.8%) with deferent opening shapes (rectangle and square), these slabs approximately have the same ultimate load capacity (about 10.71% and 12.5% from control slab S2.0) and approximately same behavior (same load-deflection behavior). This is may be because of the same amount of concrete and reinforcement steel are cut in the least critical zone (far from the intersection of two column strips)

In Group III (different slab thickness) with the same reduction in opening areas of about 4.9% with respect of control slabs, the results showed that the ultimate load capacity is directly proportional with slab thickness because of the increasing of the slab inertia, as it is shown in Fig. 6 and tabulated in Table III.

By introducing opening with the same opening area but in different location (center and corner) as in group IV (S4.1 and S4.2), the ultimate load capacity decreased by about 4% and 10 %, respectively in a comparison with the control slab without opening S4.0. Hence, it was concluded that the location of the opening has a great effect on the ultimate load capacity and the deflection. The effect of the opening which localized in the corner is much greater than that in the center as it is located in the maximum stresses zone, as it is shown in Fig. 7 and Table III.

TABLE III
TEST RESULTS OF UN-STRENGTHENED SLABS

Group	Slab No	Crack load (KN)			ultimate loading (KN)			Max. deflection (mm)		
		exp.	num.	%	exp.	num.	%	exp.	num.	%
I	**S1.0**	57.5	60	104	70	72	103	45	47	104
	S1.1	----	31.5	----	-----	37	-----	-----	28	------
	S1.2	28	30	107	35	36.5	104	33	34.8	105
	S1.3	----	28.7	----	----	31	----	----	36	----
II	**S2.0**	24.17	25	103	26.7	28	101	17.3	18.9	109
	S2.1	----	22	----	----	25	-----	-----	19.5	------
	S2.2	----	22	----	----	24.5	----		18.3	------
	S3.0.1	----	87	----	----	107	----	----	52.4	----
	S3.1.1	----	87	----	----	100	----	----	57.8	----
	S3.0.2	----	83	----	----	90	----	----	65.4	----
	S3.2.2	----	84	----	----	90	----	----	68.3	----
	S3.0.3	----	82	----	----	87	----	----	75.6	----
	S3.3.3	----	82	----	----	85	----	----	80	----
	S3.0.4	----	73	----	----	76.3	----	----	88.7	----
	S3.4.4		69.6			73.5			90	
IV	**S4.0**	----	90.5	----	----	100	----	----	57.8	----
	S4.1	----	88	----	----	96	----	----	63.8	----
	S4.2	----	76	----	----	90	----	----	68.3	----

B. Failure Load

Figs. 8-11 show the relationships between the investigated parameters and the resulted ultimate loads. Fig. 8 illustrates the relationship between the area of opening and the ultimate load, it displays that the area of opening is inversely proportional to the ultimate load, there is a reduction in the ultimate load of opening slabs S1.1, S1.2, S1.3 comparing with the control slab 48.7%, 49.3% and 56.1%, respectively. This may be caused because of the reduction of the bearing area of the slab. It was observed that opening areas which range from 100 cm^2 to 400 cm^2 nearly have the same reduction of the ultimate loads. Fig. 9 displays the relationship between the shape of opening (with the same opening area) and the ultimate load. The results showed that the shape of slab opening has a weak impact on the resulted ultimate loads. Fig. 10 presents the relationship between slab thickness and the ultimate load. It is very clear that the slab thickness is directly proportional to the ultimate load. This may be interpreted due to the increase in the slab stiffness that increases the capacity of the slab to carry loads. The relationship between position of the slab opening and the ultimate load is introduced in Fig. 11. It shows that the reduction of the ultimate load in case of the place at the corner is more than that at the center. That is because the opening in the center is in the maximum value of the moment region.

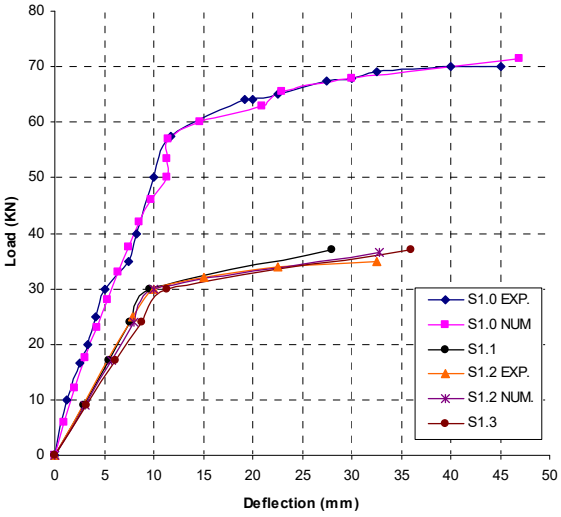

Fig. 4 Load-deflection curve of Group I

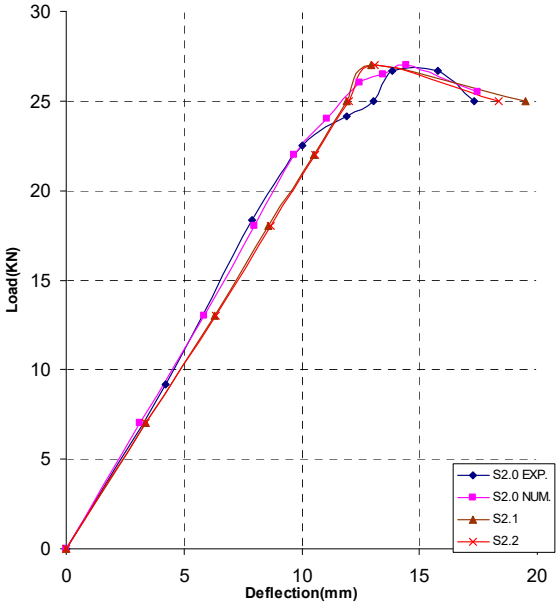

Fig. 5 Load-deflection curve of Group II

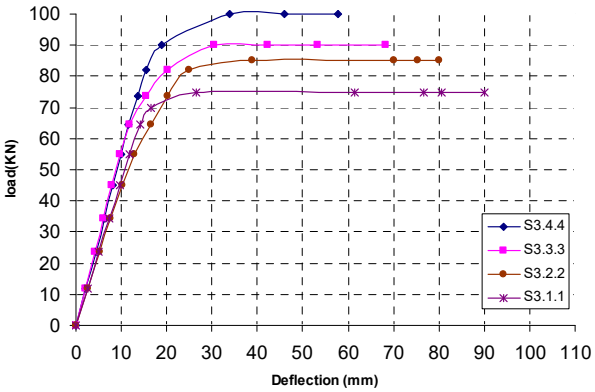

Fig. 6 Load-deflection curve of Group III

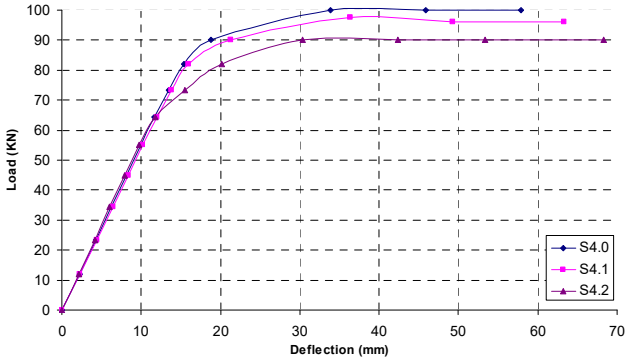

Fig. 7 Load-deflection curve of Group IV

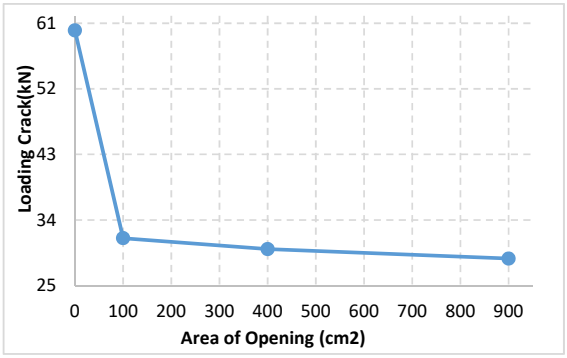

Fig. 8 The relationship between loading crack and area of opening

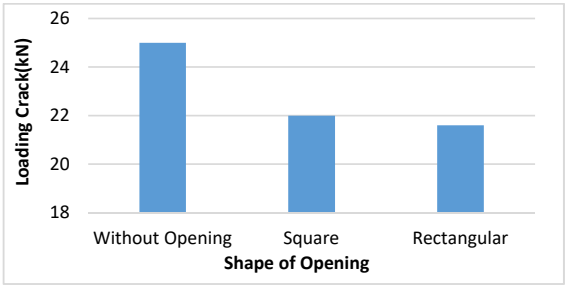

Fig. 9 The relationship between loading crack and shape of opening

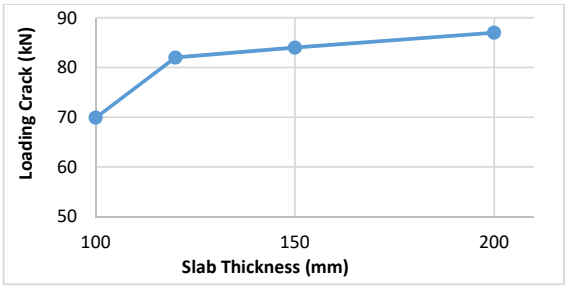

Fig. 10 The relationship between loading crack and slab thickness

C. Max. Deflection

Figs. 12-15 show the maximum deflection where it was measured at the center of the slab. It is noted that the maximum deflection is near to the opening and it has decreased gradually far from the opening.

The maximum deflection is measured in mid-span is 47.0 mm, 28.0 mm, 34.8 mm, and 36.0 mm under the ultimate loads of about 72.0 kN, 37.0 kN, 36.5 kN, and 31.0 kN for the slabs S1.0, S1.1, S1.2 and S1.3 respectively, whilst for Group II, the maximum deflection which is measured in the mid-span is 18.9 mm, 19.5 mm, and 18.3 mm under the ultimate loads of about 28.0 kN, 25.0 kN, and 24.5 kN for the slabs S2.0, S2.1, and S2.2 respectively. Because the same amount of concrete and reinforcement steel is cut in the least critical zone (far from the intersection of two column strips), also Group III, the maximum deflection is measured in mid-span is 52.4 mm, 57.8 mm, 65.4 mm, 68.3 mm, 75.6 mm, 80.0 mm, 88.7 mm, and 90.0 mm under the ultimate loads of about 107.0 kN, 100.0 kN, 90.0 kN, 90 kN, 87.0 kN 85.0 kN, 76.3 kN, and 73.5 kN for slabs S3.0.1, S3.1.1, S3.0.2, S3.2.2, S3.0.3, S3.3.3, S3.0.4, and S4.4.4 respectively because of the increasing of the slab inertia and for Group IV, the maximum deflection measured is in mid-span is 57.8 mm, 63.8 mm and 68.3 mm under the ultimate load of about 100.0 kN, 96.0 kN, and 90.0 kN for the slabs S4.0, S4.1, and S4.2, respectively because S4.1 is located in the intersection between two middle strips while S4.2 is located in the region bounded by two column strips.

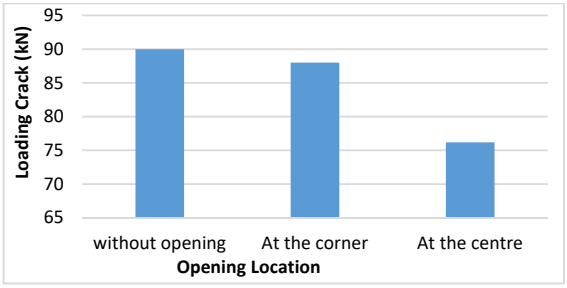

Fig. 11 The relationship between loading crack and place of opening

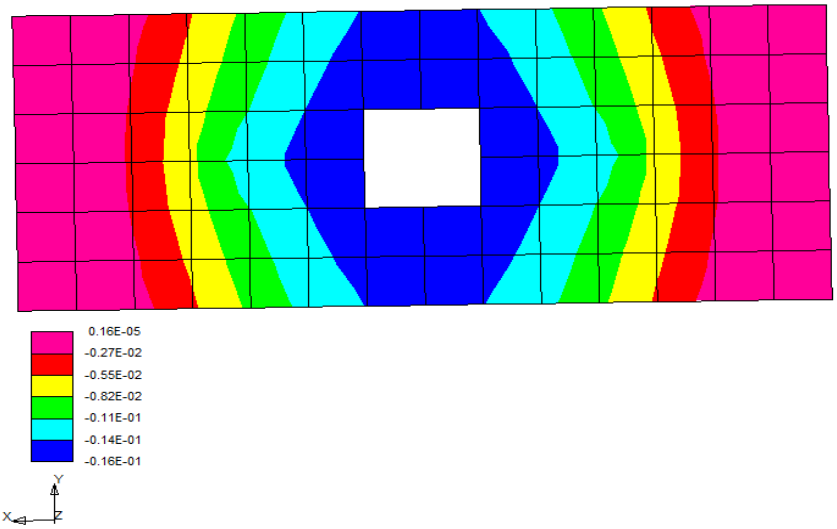

Fig. 12 The deflection mode of S1.2

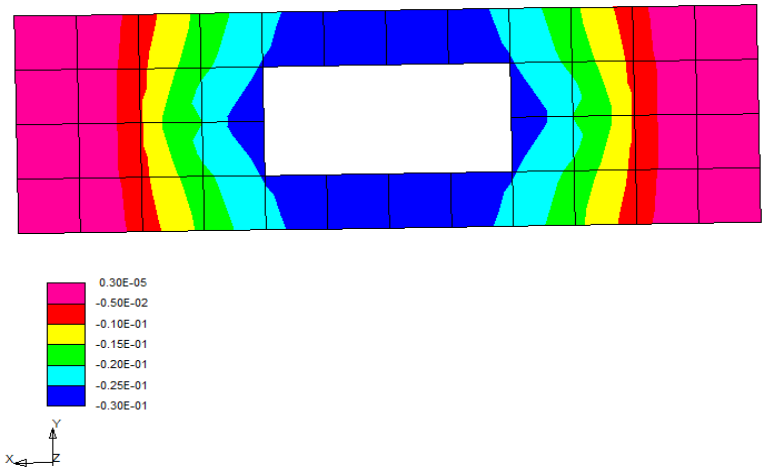

Fig. 13 The deflection mode of S2.1

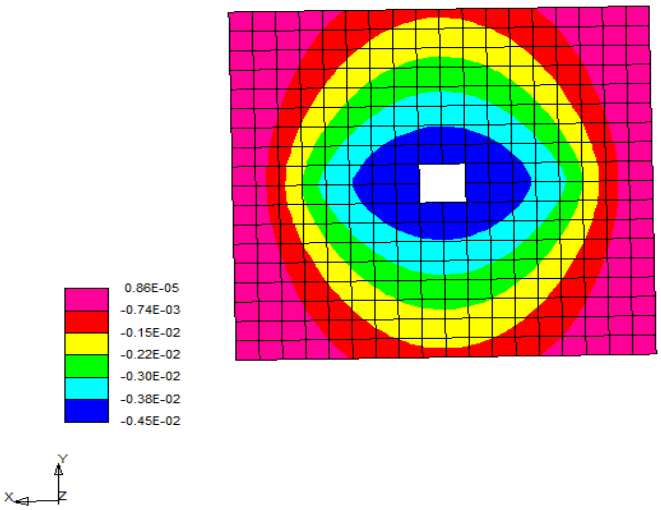

Fig. 14 The deflection mode of 3.2.2

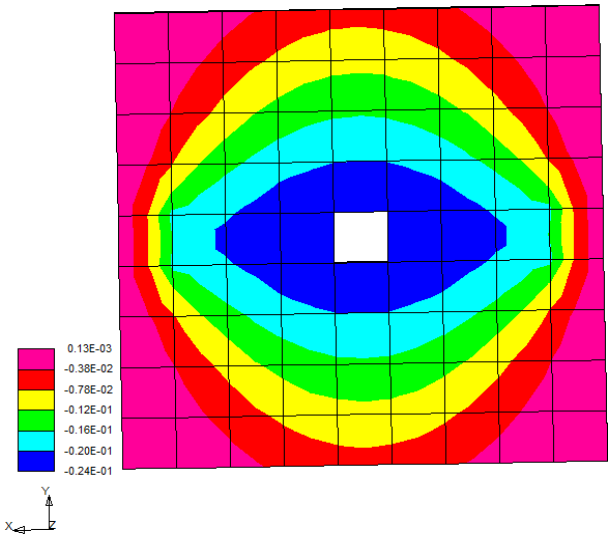

Fig. 15 The deflection mode of S3.4.4

D.Induced Stresses

In this research, the slabs with and without openings are also evaluated for the applied loads at which the slab shows first crack. The variations in load carrying capacity of the slabs are tabulated in Table III. It is obviously that the existence of opening has reduced the load carrying capacity of slab. The results also show that the first crack occurs at the edge of the opening, after that the crack is mainly concentrated at the slab edges of slab, it is followed by a concentration in stresses values at the edges of the slab, that is because the area of slab on which load is applied decreases as the size of opening increases and henceforth the load transferring is mainly concentrated at the edge of slab. The value of stresses and damage besides the opening also depends on the case of loading, supporting case, opening size and the shape of opening. For Group I, the stresses are increased by 9.7%, 29.7% and 47.8% for the slabs S1.1, S1.2, and S1.3 respectively comparing with the control slab (without opening) S1.0, while for Group II, the stresses are increased by 10.7% and 11.4 % for the slabs S2.1 and S2.2 respectively comparing with the control slab S2.0, for Group III, it is concluded that the thickness is directly affected proportional with the loading capacity of RC slabs with a square opening of thickness (150mm, 120mm and 100mm) which are less than of RC slab with a square opening of thickness 200 mm by about 10.0%, 15.0, and 26.5%, respectively; due to the increasing of its inertia. Lastly for Group IV, the stresses are increased by 30.25% and 6.4% for the slabs S4.1 and S4.2 respectively comparing with the control slab S4.0. Figs. 16- 20 show the stress concentration around the opening.

E. Damage Evolution

The dominant failure mode for RC slabs with opening is the flexural failure. The failure was due to the propagation of

cracks near the opening tip, while major cracks evolved from the opening corners and propagated towards the corners of the slab. Figs. 16-20 illustrate the damage concentration near to the opening where the moment values are expected to be maximum.

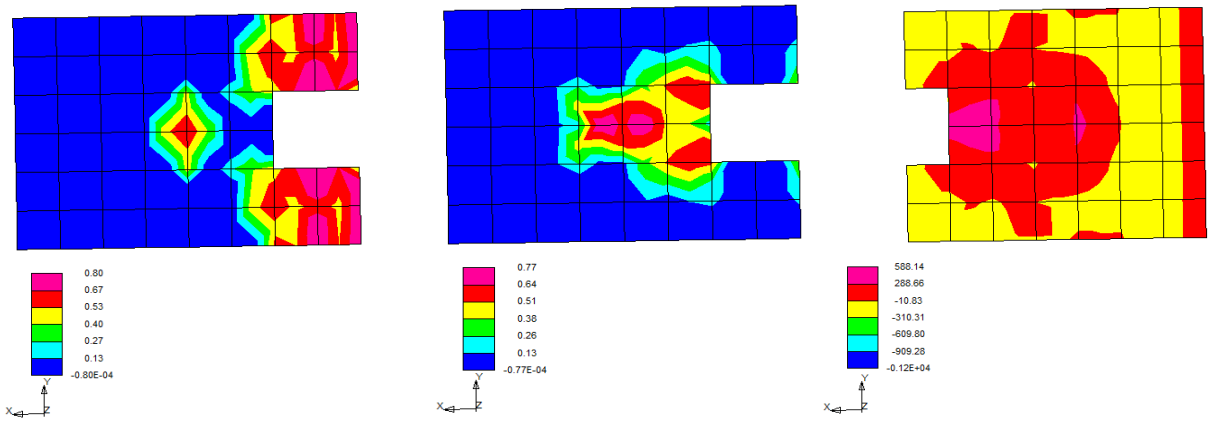

(a) (b) (c)

Fig. 16 The analysis of S11 (a) the damage values in the direction of X, (b) the damage in the direction of Y and (c) the stress values in the direction of Y

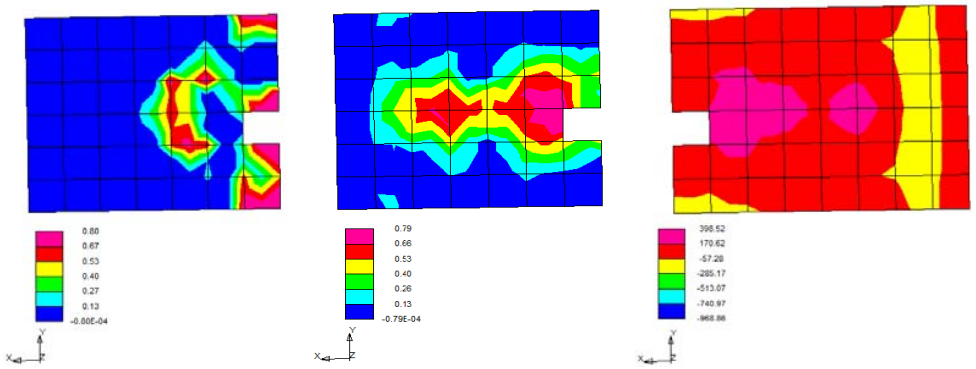

(a) (b) (c)

Fig. 17 The analysis of S12 (a) the damage values in the direction of X, (b) the damage in the direction of Y and (c) the stress values in the direction of Y

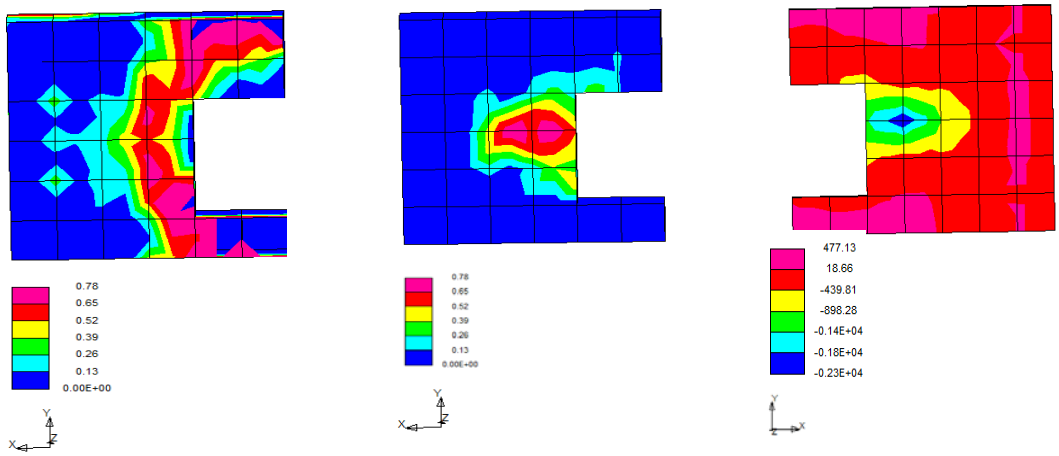

(a) (b) (c)

Fig. 18 The analysis of S13 (a) the damage values in the direction of X, (b) the damage in the direction of Y and (c) the stress values in the direction of Y

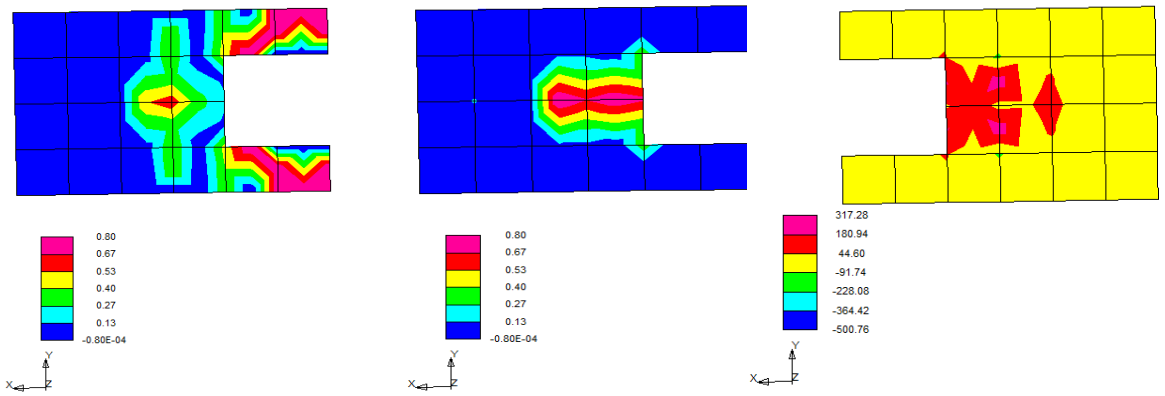

(a) (b) (c)

Fig. 19 The analysis of S21 (a) the damage values in the direction of X, (b) the damage in the direction of Y and (c) the stress values in the direction of Y

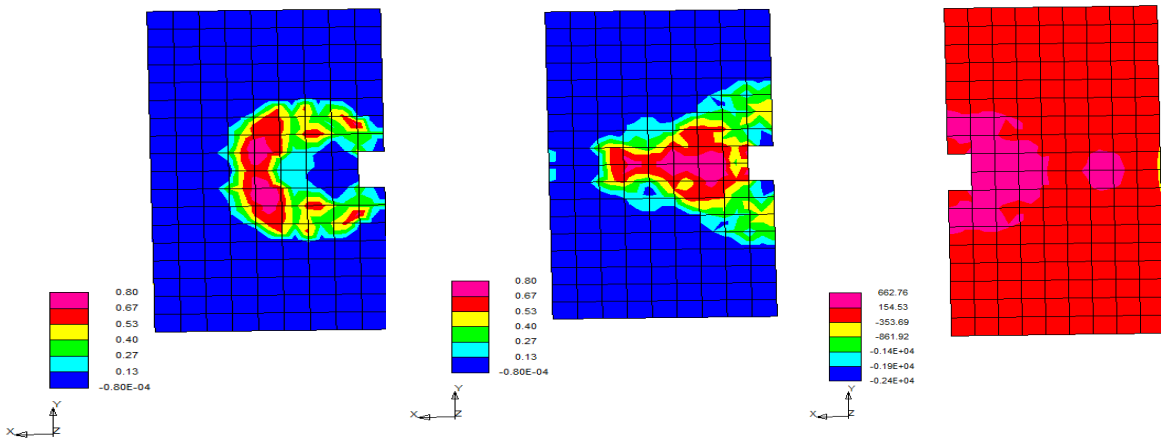

(a) (b) (c)

Fig. 20 The analysis of S3.1.1 (a) the damage values in the direction of X, (b) the damage in the direction of Y and (c) the stress values in the direction of Y

VI. Conclusion

In the recent work, a modified anisotropic nonlinear elastic damage model has been presented based on the principles of both continuum damage mechanics within the framework of the irreversible thermodynamics. This work has been built to be a simplified and effective tool for structural analysis purposes. And the following conclusions can be drawn, as:

1) The simplified continuum damage model presents the main features of RC with and without opening with a fair accuracy in comparison with the experimental results.
2) The proposed non-linear elastic damage theory in this paper has the ability to simulate the non-linearity of the deteriorated concrete structures.
3) The numerical modes of failure and strength predictions were compared with experimental measurements; it was shown that the predictions are conservative, and errors are acceptable as the model overemphasizes the values of the ultimate load of the tested slabs by 3-4%.
4) The numerical modes of failure and strength predictions were compared with experimental measurements; it was shown that the predictions are conservative, and errors are acceptable as; the model overemphasizes the values of the ultimate load of the tested slabs by 3-4%.
5) The ultimate load capacity of RC slabs with opening ratio 1.4%, 5.7% and 12.8% is less than RC without opening by about 48.7%, 49.3% and 56.1%.
6) With increasing the opening area, dramatic damage propagation occurred around the opening.
7) The numerical damage model showed that there was a significant stress concentration occurred at the corner of the opening.

References

[1] K. H. Boon, Abu Bakr M. Diah and L. Y. Loon, "Flexural behavior of reinforced concrete slabs with opening," in *Malaysian Technical Universities Conference of Engineering and Technology ,MUCEET*, June 2009.
[2] O. Enochsson, "CFRP strengthening of concrete slabs with and without opening," PhD dissertation, *Lulea University*, Sweden, 2005.
[3] Wissam D. Salman, "Strengthening of Reinforced Concrete One-Way Slabs with Opening using CFRP Strip in Flexural," *International Journal of Science and Technology* (ISSN: 2319-7064), 2013.

[4] Hossam A. Daham, "Analytical study of reinforced concrete with and without opening have different boundary conditions," *Journal of Al-Rafidien*, 2010.
[5] Chee Khoon Ng. Timothy Julius Edwarad and Daniel Kim Tee Lee, "Theoretical Evaluation on Effects of Ultimate Load-Carrying Capacity of Square Slabs" Electronic Journal of Structure Engineering, 2008.
[6] Anjaly Somasekhar and Preetha Prabhakaran," Analytical Investigation on Performance of Stiffened Waffle Slabs with Openings, Journal of Mechanical and Civil Engineering, ISSN 2278-1684, 2013.
[7] H. Madkour, "Modelling of damage-plasticity for concrete and its application for tunneling," PhD dissertation Innsbruck University, Austria, 2004.
[8] H. Madkour, "Non-linear analysis of Strengthened RC beams with web opening)," Proceeding in *International Journal of Civil Engineers, ICE, 2008*.
[9] J. L. Chaboche, "Une loi differenetielle d'endommagement de fatigue avec cumulation non lineaire," Rev. Fr. Mech., 50, 51, 1974.
[10] A. Dragon, D. Pham, P. Charles and J. F. Shao, "A model of anisotropic damage by micro-crack growth," *Proceeding of the International Symposium on Assessment and Prevention of Failure Phenomena in Rock Engineering*, 71-78. Istanbul, Turkey, 1993.
[11] J. W. Ju, "On energy based coupled elastoplastic damage theories: Constitutive modeling and computational aspects," *International Journal of Solids and Structures,* 25, 7, 803-833, 1989.
[12] W. Zhang, "Numerical analysis of continuous damage mechanics," PhD dissertation, School of Civil Engineering University of New South Wales, Australia, 1992.
[13] S. Murakami and K. Hayakawa , "Space of damage conjugate force and damage potential of elastic-plastic-damage materials," *International Journal of Damage Mechanics,* 6, 27-44, 1997.
[14] C. K. Valanis, "A Theory of damage in brittle materials," *Engineering Fracture Mechanics,* 36, 403-416, 1990.
[15] Program system FINAL- Finite element analyses program for linear and nonlinear structures 2016; Version 7.3.
[16] Yeol Choi, Ik Hyun Park, Sang Goo Kang and Chang-Geun Cho, "Strengthening of RC slabs with Symmetric Openings Using GFRP Composite Beams," *Journal of Polymers,* Vol.5, Issue 4, 2013.